Statistical Mechanics of Developable Ribbons

L. Giomi[1,2] and L. Mahadevan[1]

[1]School of Engineering and Applied Sciences, Harvard University, Cambridge, Massachusetts 02138, USA
[2]Martin A. Fisher School of Physics, Brandeis University, Waltham, Massachusetts 02454, USA

(Received 23 February 2010; published 11 June 2010)

We investigate the statistical mechanics of long developable ribbons of finite width and very small thickness. The constraint of isometric deformations in these ribbonlike structures that follows from the geometric separation of scales introduces a coupling between bending and torsional degrees of freedom. Using analytical techniques and Monte Carlo simulations, we find that the tangent-tangent correlation functions always exhibit an oscillatory decay at any finite temperature implying the existence of an underlying helical structure even in the absence of a preferential zero-temperature twist. In addition, the persistence length is found to be over 3 times larger than that of a wormlike chain having the same bending rigidity. Our results are applicable to many ribbonlike objects in polymer physics and nanoscience that cannot be described by the classical wormlike chain model.

DOI: 10.1103/PhysRevLett.104.238104 PACS numbers: 87.10.Pq, 82.35.Lr, 82.35.Pq

A shell or plate is a body whose two dimensions are comparable to each other and much larger than the third. A rod, on the other hand, is a body whose two dimensions are comparable to each other and much smaller than the third. In each of these objects, this separation of scales leads to constraints and an energetic ordering of the different possible deformations such as bending, twisting, stretching and shearing, and there are well accepted continuum and statistical theories of their behavior. There is, finally, an intermediate class of objects where all three dimensions are widely separated from each other, which we call strips or ribbons.

An example of such a chimeric object is a rectangular sheet of paper of large aspect ratio (see Fig. 1); its thickness is much smaller than its width which is itself much smaller than its length. The nanoscale world offers a number of compelling examples of these ribbonlike structures such as DNA, the secondary structures of proteins such as α helices and β sheets, carbon (graphene) and molybdenum ribbons, etc. A classical theoretical approach to the study of these filamentous objects is embodied in the wormlike chain (WLC) model [1], in which the polymer is assumed to have an inextensible backbone, but with a flexibility governed by the persistence length ℓ_p which expresses the exponential rate of decay of a tangent-tangent correlation function. Its relative simplicity and precision in describing the entropic elasticity of many semiflexible polymers has made it very attractive as an object of theoretical study. However, the accuracy of the WLC model for finite width biopolymers is still debated and a number of alternatives have been proposed to account for the torsional rigidity, the excluded volume and other features associated with a finite width [2–4]. In this Letter we consider a model for the statistical mechanics of ribbonlike objects based on a classical geometric formulation of developable surfaces. In the limit when the thickness of a ribbon is much less than its width which is itself much less than its length, we can define a center line. Then isometric deformations of the ribbon (i.e., those that preserve local distances so that the metric tensor is always Euclidean, $g_{ij} = \delta_{ij}$) can be described in terms of the orientation of the generators of the developable surface relative to the center line [5] and account for the finite width of the ribbon. Because of its tensorial nature, developability strongly constrains the allowable deformations of a ribbon in a fundamentally different way than other milder constraints such as the "railway-track" models of polymers [3]. The most striking consequence of this, illustrated in Fig. 1, is that a developable ribbon can bend without twisting but cannot twist without bending, which as we shall see has far reaching consequences.

To characterize a ribbon, we first consider the geometry of its center line in terms of the Frenet frame $(\mathbf{t}, \mathbf{n}, \mathbf{b})(s)$ of the tangent, normal and binormal vector at each point along the curve parametrized by arc-length coordinate s [6]. This orthogonal triad evolves in space according to the Frenet-Serret equations:

$$\mathbf{t}' = \kappa\mathbf{n}, \qquad \mathbf{n}' = -\kappa\mathbf{t} + \tau\mathbf{b}, \qquad \mathbf{b}' = -\tau\mathbf{n},$$

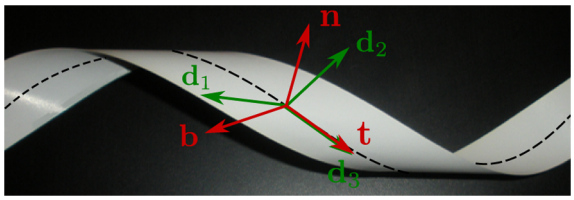

FIG. 1 (color online). A twisted paper ribbon. In presence of twist the ribbon necessarily develops a nonzero curvature, as required by the Sadowsky functional. The Frenet frame $(\mathbf{t}, \mathbf{n}, \mathbf{b})$ and the material frame $(\mathbf{d}_1, \mathbf{d}_2, \mathbf{d}_3)$ are sketched in red and green, respectively. For a developable ribbon, the two frames coincide, so that the twist of the material frame and the torsion of the center line are identical.

where κ, τ are the curvature and torsion of the space curve and the prime denotes the derivatives with respect to s. In physical ribbons, there is another distinguished frame, the material frame which is attached to each cross section; the spatial rate of rotation of this material frame is known as the twist τ_e and is not the same as the torsion of the geometric center line. For example, an arbitrary twisted ribbon can have a straight center line, while a helically wound telephone cord may only have torsion and no twist. However, when the ribbon is deformed isometrically, the direction perpendicular to the center line, which points along the binormal, also points along a material axis that corresponds locally to the only direction in which bending is possible, so that the Frenet frame and the material frame coincide and $\tau = \tau_e$. Equivalently, the projection of the curvature of the center line on the material frame always vanishes in the infinitely stiff direction.

The elastic energy due to isometric deformations of a naturally flat sheet of thickness h is given by the functional: $F = \frac{1}{2} D \int dA(\kappa_1 + \kappa_2)^2$, where κ_1 and κ_2 are the principal curvatures, $D = h^3 E/[12(1-\nu^2)]$ is the bending rigidity, E the Young modulus of the material and ν its Poisson ratio. The assumption of developability allows one to reduce the two-dimensional integral to a one-dimensional integral along the center line of the strip [7,8]:

$$F = \frac{1}{2} D \int_0^L ds \frac{(\kappa^2+\tau^2)^2}{\kappa'\tau - \kappa\tau'} \log\left[\frac{\kappa^2 + \frac{w}{2}(\kappa'\tau - \kappa\tau')}{\kappa^2 - \frac{w}{2}(\kappa'\tau - \kappa\tau')}\right],$$

where κ and τ are, respectively, the curvature and the torsion of the center line, w is the lateral width of the ribbon, and L the length of the center line. In the limit $w/L \ll 1$ this yields the Sadowsky functional [5]:

$$F = \frac{1}{2} Dw \int_0^L ds \frac{(\kappa^2+\tau^2)^2}{\kappa^2}. \quad (1)$$

As anticipated, the nonlinear coupling between curvature and torsion in (1) implies that an inextensible ribbon can bend without twisting ($\tau = 0$, $\kappa \neq 0$), but cannot twist without bending ($\tau \neq 0 \longrightarrow \kappa \neq 0$).

To make the Sadowsky's functional (1) amenable to numerical simulation of a discretized analog, we consider a chain of $N = L/a$ consecutive vertices $\mathbf{x} = \{\mathbf{x}_1, \mathbf{x}_2, \ldots, \mathbf{x}_N\}$ separated by a fixed length a. At each point $\mathbf{x}_i$ in the chain, the discrete Frenet frame is given by: $\mathbf{F}_i = (\mathbf{t}_i, \mathbf{n}_i, \mathbf{b}_i)$. $\mathbf{F}_i$ are orthogonal 3×3 matrices whose columns are given by the column vectors $\mathbf{t}_i$, $\mathbf{n}_i$, and $\mathbf{b}_i$. Calling θ_i and ϕ_i the angles formed by consecutive tangent and binormal vectors (i.e., $\mathbf{t}_i \cdot \mathbf{t}_{i-1} = \cos\theta_i$ and $\mathbf{b}_i \cdot \mathbf{b}_{i-1} = \cos\phi_i$), the Frenet equations for the moving trihedron are expressed as $\mathbf{F}_i = \mathbf{F}_{i-1}\mathbf{R}_i$ [9], where

$$\mathbf{R}_i = \begin{pmatrix} \cos\theta_i & -\sin\theta_i & 0 \\ \sin\theta_i \cos\phi_i & \cos\theta_i \cos\phi_i & -\sin\phi_i \\ \sin\theta_i \sin\phi_i & \cos\theta_i \sin\phi_i & \cos\phi_i \end{pmatrix}. \quad (2)$$

We note that $\mathbf{t}_i \cdot \mathbf{n}_{i-1} = \sin\theta_i \cos\phi_i$ and $\mathbf{t}_i \cdot \mathbf{b}_{i-1} = \sin\theta_i \sin\phi_i$. Thus θ_i and ϕ_i are also the polar and azimuthal angle of a system of spherical coordinates (see inset of Fig. 2). The discrete analog of curvature and torsion can be easily found $\kappa_i^2 = a^{-2}|\mathbf{t_i} - \mathbf{t}_{i-1}|^2 = 2a^{-2}(1-\cos\theta_i)$ and $\tau_i^2 = a^{-2}|\mathbf{b_i} - \mathbf{b}_{i-1}|^2 = 2a^{-2}(1-\cos\phi_i)$. The energy (1) can thus be written as:

$$\frac{F}{k_B T} = \beta \sum_{i=1}^{N} \frac{[(1-\mathbf{t}_i \cdot \mathbf{t}_{i+1}) + (1-\mathbf{b}_i \cdot \mathbf{b}_{i+1})]^2}{(1-\mathbf{t}_i \cdot \mathbf{t}_{i+1})}, \quad (3)$$

where $\beta = Dw/(ak_BT)$. This serves as a starting point for Monte Carlo simulations of a chain composed of N segments of unit length and its conformation is updated using pivot moves through a METROPOLIS algorithm. For every chain we perform 10^6 Monte Carlo sweeps, the first half of which is devoted to equilibration. Figure 3 shows the tangent-tangent and binormal-binormal correlation for a chain of $N = 100$ segments at various temperatures. We see that while $\langle \mathbf{b}_n \cdot \mathbf{b}_0 \rangle$ always exhibits exponential decay, $\langle \mathbf{t}_n \cdot \mathbf{t}_0 \rangle$ has oscillations superimposed on an exponential decay. Upon raising the temperature, the frequency increases, but the exponential damping becomes stronger.

To understand this result, we first derive the tangent-tangent and binormal-binormal correlation functions from the iterated transfer matrix: $\langle \mathbf{t}_n \cdot \mathbf{t}_0 \rangle = \langle \mathbf{R}_1 \mathbf{R}_2 \ldots \mathbf{R}_n \rangle_{11}$ and $\langle \mathbf{b}_n \cdot \mathbf{b}_0 \rangle = \langle \mathbf{R}_1 \mathbf{R}_2 \ldots \mathbf{R}_n \rangle_{33}$ [4], noting that since the energy (3) is a sum over individual segments, the Boltzmann measure $\exp(-F/k_BT)$ is factorizable and $\langle \mathbf{R}_1 \mathbf{R}_2 \ldots \mathbf{R}_n \rangle = \langle \mathbf{R} \rangle^n$. Moreover, for sufficiently large spatial separation the behavior of the correlation functions will be dictated by the largest eigenvalue in the spectrum of $\mathbf{R}$. Assuming $\langle \sin\phi \rangle = 0$, the transfer matrix $\mathbf{R}$ becomes block diagonal and the eigenvalues are given by the roots of the characteristic equation $\lambda^2 - b\lambda + c = 0$ with $b = \langle \cos\theta \rangle + \langle \cos\theta \cos\phi \rangle$ and $c = \langle \cos\theta \rangle \langle \cos\theta \cos\phi \rangle + \langle \sin\theta \rangle \langle \sin\theta \cos\phi \rangle$, so that

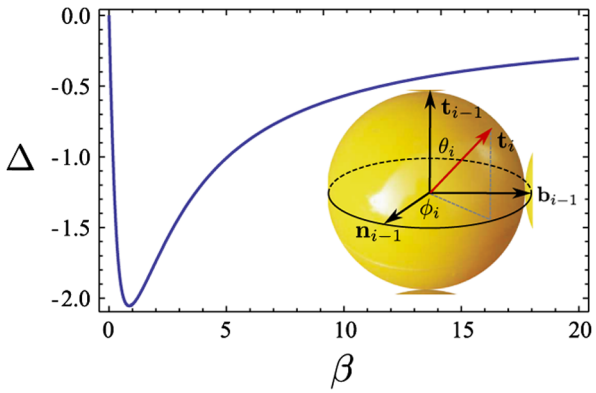

FIG. 2 (color online). The quantity Δ defined in the text as a function of β, calculated from the exact integral expression given on the last page. With exception for the two limits $\beta \to 0, \infty$, Δ is always negative and the associated eigenvalues $\lambda_{1,2} = \frac{1}{2}(b \pm \sqrt{\Delta})$ are complex and conjugate. In the inset the discrete Frenet frame.

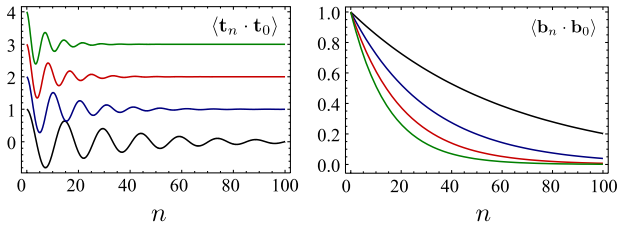

FIG. 3 (color online). Tangent-tangent (left) and binormal-binormal (right) correlation functions from Monte Carlo simulations of a polymer chain of $N = 100$ segments at $T = 0.1$ (black), 0.2 (blue), 0.3 (red) and 0.4 (green). The graphs of $\langle \mathbf{t}_n \cdot \mathbf{t}_0 \rangle$ have been translated along the vertical axis to avoid overlaps.

$$\lambda_{1,2} = \frac{b \pm \sqrt{\Delta}}{2}, \qquad \lambda_3 = \langle \cos\phi \rangle,$$

where $\Delta = b^2 - 4c$. Thus the binormal-binormal correlation function always exhibits exponential decay:

$$\langle \mathbf{b}_n \cdot \mathbf{b}_0 \rangle = e^{-s/\ell_\tau}, \tag{4}$$

where $\ell_\tau^{-1} = -a^{-1} \log\langle \cos\phi \rangle$ is the torsional persistence length and $s = na$. On the other hand, the sign of Δ dictates the behavior of the tangent-tangent correlation function. When $\Delta > 0$, the eigenvalues $\lambda_{1,2}$ are real and $\langle \mathbf{t}_n \cdot \mathbf{t}_0 \rangle$ has the typical exponential decay of a WLC. When $\Delta < 0$ the eigenvalues are complex and $\langle \mathbf{t}_n \cdot \mathbf{t}_0 \rangle$ has the form:

$$\langle \mathbf{t}_n \cdot \mathbf{t}_0 \rangle = e^{-s/\ell_p} \cos ks, \tag{5}$$

with $k = a^{-1} \arctan(\sqrt{-\Delta}/b)$ and $\ell_p^{-1} = -\frac{1}{2} a^{-1} \log c$. An exact numerical calculation of Δ, shown in Fig. 2 as a function of β, shows it is always negative so that the tangent-tangent correlation function is always oscillatory at any nonzero temperature.

This oscillatory behavior is reminiscent of spin chains with competing ferromagnetic and antiferromagnetic interactions. In these systems the oscillatory behavior of the two-point correlation functions denotes the existence of a *helical phase* in which the magnetization varies periodically in space. The critical point that divides the disorder phase and the helical phase is traditionally referred to as "Lifshitz point" [10]. Analogously, an oscillating tangent-tangent correlation function in our polymer model implies the presence of an underlying helical structure that persists at any finite temperature even in absence of a spontaneous twist, i.e., so that the Lifshitz point here is $T = \infty$. In Fig. 4 we show that our numerical simulations capture this feature, due to the strong geometrical constraint of developability; i.e., the ribbon is isometric to a flat strip at *any* temperature, and thus bends when twisted. The notion of Lifshitz point has been previously used to describe the low temperature phase of a "railway-track" polymer consisting of two parallel WLCs connected by a rigid bond [3]. This phase is marked by an oscillatory binormal-binormal correlation function which results in a "rod-kink" structure in which the ribbon is at every point along its contour either twisted and unbent (rod) or bent and untwisted (kink). This is qualitatively different from our results where it is impossible for the ribbon to be twisted and unbent simultaneously, due to the fact that the constraint of developability is implemented exactly in Eq. (1), unlike in any previous attempts.

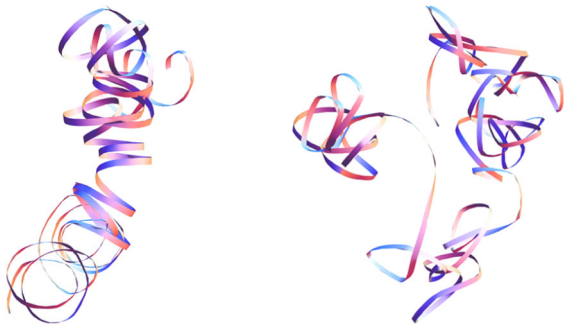

FIG. 4 (color online). The typical conformation of a ribbonlike polymer after 10^6 Monte Carlo iterations. (Left) $\beta^{-1} = 0.1$ and (right) $\beta^{-1} = 1$. At low temperature the ribbon fluctuates around an underlying helical shape. The radius and the pitch of the helix are set by the persistence length ℓ_p and the wave number k and are proportional to βa and $\beta^{1/2} a$, respectively.

Next we give an analytical estimate of the three relevant quantities ℓ_p, ℓ_τ and k in the low temperature regime. The partition function for the ribbon is given by $Z = z_1^N$ with:

$$z_1 = \int \frac{d\Omega}{4\pi} e^{-(1/2)\beta a^2(\kappa^2 + 2\tau^2 + \tau^4/\kappa^2)}, \tag{6}$$

with $d\Omega = d\phi d\theta \sin\theta$ the infinitesimal solid angle. The analytical calculation of thermal average is complicated by the coupling term between curvature and torsion, but this can be removed by rewriting the τ^4/κ^2 term as a Gaussian integral of the form:

$$e^{-\beta a^2 \tau^4/2\kappa^2} = \left(\frac{\beta a^2 \kappa^2}{2\pi}\right)^{1/2} \int_{-\infty}^{\infty} dy e^{-(1/2)\beta a^2(\kappa^2 y^2 + 2i\tau^2 y)}. \tag{7}$$

With this substitution, curvature and torsion are now decoupled and the single-node partition function reads:

$$z_1 = \left(\frac{\beta}{\pi}\right)^{1/2} \int_{-\infty}^{\infty} dy \int \frac{d\Omega}{4\pi} (1 - \cos\theta)^{1/2} e^{-\beta[\lambda(1-\cos\theta) + \mu(1-\cos\phi)]}, \tag{8}$$

with $\lambda = (1 + y^2)$ and $\mu = 2(1 + iy)$, so that the ribbon is equivalent to a wormlike polymer with finite but complex-valued bending and torsional stiffness. Calculating the solid-angle integral in the previous expression yields

$$z_1 = \left(\frac{\beta}{4\pi}\right)^{1/2} \int_{-\infty}^{\infty} dy \frac{e^{-\beta\mu} I_0(\beta\mu)\gamma(\frac{3}{2}, 2\beta\lambda)}{(\beta\lambda)^{3/2}}, \quad (9)$$

where I_0 and γ are, respectively, the modified Bessel function of zeroth order and the incomplete gamma function [11]. Analogously one can calculate the ensemble average $\langle\cdot\rangle = z_1^{-1} \int \frac{d\Omega}{4\pi} (\cdot) e^{-(1/2)\beta a^2(\kappa^2+2\tau^2+\tau^4/\kappa^2)}$ which yields:

$$\langle \cos\theta \cos m\phi \rangle = \left(\frac{\beta}{4\pi}\right)^{1/2} z_1^{-1} \int_{-\infty}^{\infty} dy e^{-\beta\mu} I_m(\beta\mu) f_1(\beta\lambda),$$

$$\langle \sin\theta \cos m\phi \rangle = \left(\frac{\beta}{4\pi}\right)^{1/2} z_1^{-1} \int_{-\infty}^{\infty} dy e^{-\beta\mu} I_m(\beta\mu) f_2(\beta\lambda),$$

where m is an integer in $\{0, 1\}$ and

$$f_1(\beta\lambda) = \frac{\gamma(\frac{3}{2}, 2\beta\lambda)}{(\beta\lambda)^{3/2}} - \frac{\gamma(\frac{5}{2}, 2\beta\lambda)}{(\beta\lambda)^{5/2}},$$

$$f_2(\beta\lambda) = \frac{3}{\sqrt{2}(\beta\lambda)^2} - \frac{\sqrt{\pi}(3 + 4\beta\lambda)}{4(\beta\lambda)^{5/2}} e^{-2\beta\lambda} \mathrm{erfi}(\sqrt{2\beta\lambda}),$$

with erfi the imaginary error function [11]. At low temperatures ($\beta \gg 1$), asymptotic expansions of the functions I_0, γ and erfi yield

$$\langle \cos\theta \cos m\phi \rangle \simeq 1 - \frac{21(1 - 4m^2)}{16\beta} + \frac{4(7 - 173m^2)}{5 + 128\beta},$$

$$\langle \sin\theta \cos m\phi \rangle \simeq \frac{128\beta[40\beta - 7(2 + m^2)] - 99(1 - 4m^2)}{12\sqrt{2\pi}\beta^{3/2}(5 + 128\beta)}$$

from which we find the persistence lengths ℓ_p and ℓ_τ

$$\ell_p = \left(\frac{75}{64} - \frac{25}{9\pi}\right)^{-1} \frac{Dw}{k_B T}, \qquad \ell_\tau = \frac{32}{5} \frac{Dw}{k_B T},$$

and the wave number k:

$$k = \frac{5}{3} \sqrt{\frac{2}{\pi a} \frac{k_B T}{Dw}}.$$

A plot of ℓ_p, ℓ_τ, and k versus temperature is shown in Fig. 5. We see that as a consequence of the geometric coupling between curvature and torsion in a developable ribbon, the persistence length is a factor $(\frac{75}{64} - \frac{25}{9\pi})^{-1} = 3.476$ larger than that of a WLC at the same temperature.

Our study has a set of clear experimental predictions for the equilibrium statistical mechanics of ribbonlike polymers where all three length scales are well separated. First, the tangent-tangent correlation function exhibits an oscillatory decay at any finite temperature, implying an underlying helical structure even in absence of any natural twist at zero temperature. For a ribbon with finite extensibility, even if the helical phase disappears at high enough temperatures, the Lifshitz point should persist but is shifted to $T = T^*$, and the mean field estimate for the oscillatory wave number $k \sim [k_B(T - T^*)/Dwa]^{1/2}$. The helical structures that arise herein are reminiscent of those found in biopolymers and proteins, and suggest a natural generalization of our theory to include short range forces that will stabilize these structures. In the presence of forces, the geometrical structure of ribbons is expected to lead to qualitative differences in the force-extension curves of these ribbons as well as in their motion, topics of future study.

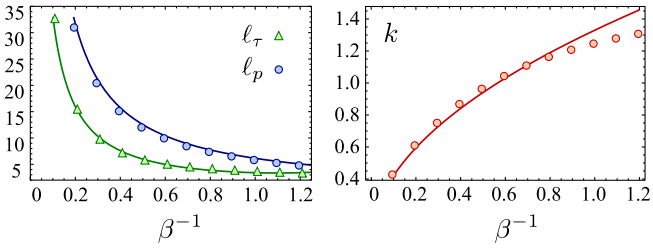

FIG. 5 (color online). Persistence length and torsional persistence length (left) as a function of β^{-1} (in units of a). (Right) Tangent-tangent correlation function wave number k (in units of a^{-1}) as a function of β^{-1}. Dots correspond to numerical data and lines to analytical predictions for the low temperature regime. For biopolymers of Young modulus $E \approx 100$ MPa, $h \approx 1$ nm and $w/a \approx 1$, the value of β^{-1} in the plots spans the temperature range $T[0, 10^3]$ K.

This work was partially supported by NSF through the Harvard MRSEC and the Brandeis MRSEC, by the Harvard Kavli Institute for Bionano Science & Technology and by the MacArthur Foundation.

[1] O. Kratky and G. Porod, Recl. Trav. Chim. Pays-Bas **68**, 1106 (1949); J. F. Marko and E. D. Siggia, Macromolecules **27**, 981 (1994).
[2] J. D. Moroz and P. Nelson, Proc. Natl. Acad. Sci. U.S.A. **94**, 14 418 (1997); Macromolecules **31**, 6333 (1998); C. Bouchiat and M. Mézard, Phys. Rev. Lett. **80**, 1556 (1998); S. Panyukov and Y. Rabin, Phys. Rev. Lett. **85**, 2404 (2000).
[3] T. B. Liverpool, R. Golestanian, and K. Kremer, Phys. Rev. Lett. **80**, 405 (1998); R. Golestanian and T. B. Liverpool, Phys. Rev. E **62**, 5488 (2000).
[4] D. Marenduzzo, C. Micheletti, H. Seyed-allaei, A. Trovato, and A. Maritan, J. Phys. A **38**, L277 (2005).
[5] M. Sadowsky, Sitzungsber. Preuss. Akad. Wiss. Phys. Math. Kl. **22**, 412 (1930).
[6] D. J. Struik, *Lectures on Classical Differential Geometry* (Dover Publications, Mineola, NY, 1988).
[7] W. Wunderlich, Monatshefte fur Mathematik **66**, 276 (1962).
[8] L. Mahadevan and J. B. Keller, Proc. R. Soc. A **440**, 149 (1993).
[9] J. R. Quine, T. A. Cross, M. S. Chapman, and R. Bertram, Bull. Math. Biol. **66**, 1705 (2004).
[10] S. Redner and H. E. Stanley, Phys. Rev. B **16**, 4901 (1977); R. M. Hornreich, R. Liebmann, H. G. Schuster, and W. Selke, Z. Phys. B **35**, 91 (1979).
[11] M. Abramowitz and I. A. Stegun, *Handbook of Mathematical Functions: With Formulas, Graphs, and Mathematical Tables*, (Dover Publications, Mineola, NY, 1996).